Cool diffusion flames of butane isomers activated by ozone in the counterflow

Adamu Alfazazi[a*], Abdullah Al-Omier[a,b], Andrea Secco[a,c], Hatem Selim[a,d], Yiguang Ju[e], S. Mani Sarathy[a*]

[a] King Abdullah University of Science and Technology (KAUST), Clean Combustion Research Center (CCRC), Thuwal 23955-6900, Saudi Arabia
[b] Department of Chemical Engineering, King Faisal University, Al-Ahsa 31982, Saudi Arabia.
[c] Università di Bologna, Dipartimento di Chimica Industriale "Toso Montanari", Viale Risorgimento 4, 40136 Bologna, Italy
[d] GE Power, Saudi GE Technology & Innovation Center, Dhahran, 34464, Saudi Arabia
[e] Department of Mechanical and Aerospace Engineering, Princeton University, Princeton, NJ 08544, USA

**Corresponding Authors:*

Adamu Alfazazi

Adamu.Fazazi@kaust.edu.sa

S. Mani Sarathy

Mani.sarathy@kaust.edu.sa

Al Kindi Building 5 Room 4336, KAUST

Thuwal, Saudi Arabia 23955

Abstract

Ignition in low temperature combustion engines is governed by a coupling between low-temperature oxidation kinetics and diffusive transport. Therefore, a detailed understanding of the coupled effects of heat release, low-temperature oxidation chemistry, and molecular transport in cool flames is imperative to the advancement of new combustion concepts. This study provides an understanding of the low temperature cool flame behavior of butane isomers in the counterflow configuration through the addition of ozone. The initiation and extinction limits of butane isomers' cool flames have been investigated under a variety of strain rates. Results revealed that, with ozone addition, establishment of butane cool diffusion flames was successful at low and moderate strain rates. Iso-butane has lower reactivity than n-butane, as shown by higher fuel mole fractions needed for cool flame initiation and lower extinction strain rate limits. Ozone addition showed a significant influence on the initiation and sustenance of cool diffusion flames; as ozone-less cool diffusion flame of butane isomers could not be established even at high fuel mole fractions. The structure of a stable n-butane cool diffusion flame was qualitatively examined using a time of flight mass spectrometer. Numerical simulations were performed using a detailed chemical kinetic model and molecular transport to simulate the extinction limits of the cool diffusion flames of the tested fuels. The model qualitatively captured experimental trends for both fuels and ozone levels, but over-predicted extinction limits of the flames. Reactions involving low-temperature species predominantly govern extinction limits of cool flames. The simulations were used to understand the effects of methyl branching on the behavior of n-butane and iso-butane cool diffusion flames.

Keywords: cool diffusion flames, counterflow, butane isomers, ozone, mass spectrometer

1. Introduction

In efforts to comply with the stringent emission regulations, auto manufacturers are investigating various combustion strategies that produce lower combustion temperatures. Such low-temperature combustion (LTC) strategies e.g. the partially premixed combustion, PPC [1] and gasoline direct injection, GDI [2] are becoming increasingly attractive as they produce less emission and improve overall engine efficiency. One of the challenges of these engines, however, is how to control the heat release during the compression stroke and thus, the ignition timing. Ignition in LTC engines often occurs in two stages, the first stage which occurs at low temperature and the second stage ignition respectively. Low-temperature cool flames and associated heat release during the first stage affects the heat release, the timing of the second stage ignition, and even knocking [3-5]. Engine studies [3-7] have shown that stratified combustion concepts display ignition phenomenon that is governed by both molecular transport and chemical kinetic processes.

The concept of LTC and controlling oxidation chemistry is well documented for different fuels in homogeneous systems such as jet stirred reactors (JSR), rapid compression machines (RCM) and shock tubes (ST) [8-14]. Many studies were carried out to understand low temperature fuel oxidation and intermediate species produced in these systems. This has influenced the understanding and advancement in building chemical mechanisms used in modeling LTC in these homogeneous systems. However, transport processes are negligible in the aforementioned homogeneous systems, and do not contribute to the evolution of cool flames and low-temperature heat release. In counterflow diffusion systems, where the fuel is initially separated from the oxidizer, the transport timescale is comparable to the reaction time scales. Therefore, both transport and kinetics contribute to the morphology and sustenance of cool flames using the opposed flow configuration [15]. These systems are canonical representations of transport-kinetic couplings present in PPC combustion engines.

Because most of previous studies focused on testing high strain rates, which require high temperature to achieve ignition [16-20], cool flame ignition in the counterflow configuration has received little attention. Nevertheless, initial pieces of evidence from the studies by Zheng et al. [21] and Grana et al. [22] involving hot diffusion flame suggested the existence of low-temperature reactivity in the counterflow flame. Later, Law et al. [23] computationally

investigated the exhibition of LTC in the counterflow using n-heptane as the fuel. They noticed the occurrence of a secondary s-curve which is controlled by low-temperature species.

Few experimental studies on low-temperature combustion have been carried out using the counterflow configuration. Sun et al. [24] and Won et al. [25] established dimethyl ether and n-heptane cool flames, respectively, using by plasma discharge and ozone sensitization. It was shown that by adding ozone to the oxidizer stream in opposed flow systems, atomic oxygen produced as a result of ozone decomposition in the preheating zone intensely reduces the initiation time scales of low-temperature chemistry [26], thereby extending the flammable region of cool diffusion flames to higher stretch rates. Species measurements of CH_2O and major reactants and intermediate species in diffusion cool flames by using laser induced fluorescence and a micro-GC showed that the existing low temperature kinetic mechanisms of n-heptane and dimethyl ether over-predicted the cool flame temperature and heat release rate. Their numerical simulations further showed that n-heptane cool diffusion flames are controlled by transport of species and low-temperature chemistry triggered by breakdown of ozone. Deng et al. [15] examined the low-temperature ignition of dimethyl ether (DME) and measured the intensities of formaldehyde species (HCHO) with the aid of infrared imaging. They provided an experimental evidence of the occurrence of such flame by applying optical detection and measurement in counterflow of heated air stream against diluted N_2/DME mixture. They used a photomultiplier (PMT) to detect the CH_2O^* chemiluminescence, which characterizes the low-temperature reaction; while sensitive infrared imaging was used to observe the ignition temperature. They revealed that low-temperature ignition is favored at low strain rates. In a separate study, Deng et al. [27] studied the extinction strain rates and ignition limit of DME/air at high pressures. They observed and quantified the existence of a hysteresis between cool flame ignition and extinction. They noted that heat release from LTC and hysteresis are largely promoted at high ambient pressure and oxygen concentrations.

The major challenge of establishing stabilized cool flames in non-premixed counterflow is the slow initiation chemistry at low temperature, which prevents the fuel from breaking down into small radicals and formaldehyde, thus preventing low-temperature branching reactions and self-initiation of the flame. In a separate study, Reuter et al. [28] compared the extinction limits of cool diffusion flames of large saturated alkanes; from n-heptane to n-tetradecane. They found that fuels with longer hydrocarbon chain lengths produce stronger cool diffusion flames, but at

low strain rates, ozone addition greatly improved the low-temperature chemistry and made the cool flame reactivity independent of the carbon chain length. In the same study, they observed that cool diffusion flames can be sustained for large alkanes at high fuel mole fractions without ozone, but doubted if ozone-less cool flames could be sustained for n-alkanes less than n-hexane.

Clearly, the experimental method proposed by Won et al. [25] facilitates the establishment of sustaining cool diffusion flames in the counterflow facility in conditions at which cool flames may not be sustained. It also provides a platform to simultaneously study the combined effect chemical kinetics, heat release and transport on low-temperature cool diffusion flames. One of the major revelations from the above studies is that the existing numerical models over-predict the measured cool flame ignition and extinction limits [25, 28-30]. This implies that the LTC is still not well developed and the current chemical kinetic models cannot accurately describe the cool flame behavior and its heat release rate, despite their capability to reproduce many homogeneous experiments at low temperatures.

With this in mind, the present study is aimed at employing the counterflow diffusion configuration assisted by ozone addition, to see if butane isomers exhibit low-temperature behavior in transport affected systems. As previously done for hot flames [20, 31, 32], this study provides an understanding of the influence of methyl branching on extinction limits and initiation of cool diffusion flames at various strain rates. Also, this study investigates the influence of both temperature and ozone concentration on the extinction limits of the tested fuels. Qualitative measurements of characteristic low temperature species as well as other species were obtained using a mass spectrometer. The mass spectrometer contains a sampling system, an ion source, a mass analyser and a detector all kept under high vacuum condition. Finally, with the aid of molecular transport and detailed chemistry, an analysis is carried out to understand the detailed structure and reactions responsible for the extinction of cool diffusion flames of butane isomers.

The choice of butane isomers as fuels cannot be over emphasized. Butane is a constituent of commercial gasoline and the simplest alkane exhibiting structural isomerism. n-Butane (RON-94) and iso-butane (RON 102) exhibit different knocking properties in spark ignition engines. Furthermore, n-butane is a simple gaseous hydrocarbon that shows a broad range of combustion properties such as negative temperature coefficient (NTC), low-temperature chain branching,

cool flame and hot flame [18]. Moreover, accurate kinetic models of butane are necessary to build oxidation mechanisms of higher hydrocarbons. A number of studies have been carried out to understand butane isomers' combustion characteristics. This led to the development of several comprehensive kinetic models for the oxidation of butane [33-39]. Nevertheless, a detailed low-temperature study of butane isomers in a non-premixed diffusive system is still not available. Therefore this study provides additional data for validation of the existing butane models.

2. Experimental and Numerical procedures

Figure 1 illustrates the counterflow configuration used in this work. The burner has of two opposing duct nozzles. Preheated Fuel/N_2 mixture is introduced into the upper nozzle, while the oxidizer is injected into the lower nozzle. The upper part of the burner consists of an alumina tube, internal diameter, d = 25 mm, directing preheated fuel stream downward. A preheater and an external Thermcraft heater (1-1/4ID, X8L, 365W, 115V, 12" braided leads) heats the fuel stream. A high temperature-resistant insulation surrounds the alumina tube to minimize radiation heat loss. The heaters are electrically controlled with variable transformers to provide constant power.

The oxidizer stream consists of oxygen and ozone. An ozone generator from Ozone Solutions (TG40) generates ozone from pure oxygen (>99.9% purity). A calibrated ozone monitor (2B Technology Model 106-H) is connected to the outlet of the ozone generator before the lower duct of the burner to enable constant and accurate measurement of ozone concentration in the oxidizer stream. This analyzer measures ozone concentration using UV light absorption with accuracy greater than 0.02wt% O_2 or 2% of measurement. Production of ozone from the ozone generator is inversely proportional to the oxygen flow rate; therefore, feed oxygen is maintained throughout all measurements to keep the concentration of ozone constant [25]. In order to ensure a constant O_3 concentration, the O_2 flow rate must be held constant at the same time, momentum balance must be achieved. The counterflow flame momentum was balanced by changing the fuel side flow rate (both nitrogen and fuel) accounting for oxidizer momentum and fuel dilution. The variation in total fuel stream flow rate is compensated by a change in the total fuel stream velocity and this is achieved by controlling both pure fuel and nitrogen volumetric flow rate, and thus a momentum balance can be achieved. Since ozone concentration in the oxidizer stream is

influenced by the volumetric flow rate of oxygen to the ozone generator, three different oxygen flow rates were tested in this experiment. To change the strain rates, the nozzles separation distance is varied.

A flow-straightening mesh is placed at the bottom of the oxidizer and fuel ducts. The upper and lower nozzles are surrounded by concentric curtain-flows to shield the flow-field from the surrounding. The two nozzles are separated by a distance, L. The strain rate, a, given by Eq. (1), a, is defined as the density-weighted gradient of the axial flow velocity [40]. The fuel flow velocity normal to the stagnation plane at the exit of the fuel nozzle and the density of the fuel stream are V_1 and ρ_1 respectively. The oxidizer flow velocity normal to the stagnation plane at the exit of the oxidizer nozzle and the density of the oxidizer stream are V_2 and ρ_2, accordingly. The accuracy of the measurement of the fuel stream temperature was determined to be ±5 K. The accuracies of the fuel mole fraction and strain rate were 3% and 5% of the recorded values, respectively. The experimental repeatability of the reported strain rate at extinction was 3% of the recorded values.

$$a = \frac{2|V_2|}{L}\left(1 + \frac{|V_1|\sqrt{\rho_1}}{|V_2|\sqrt{\rho_2}}\right)$$

Numerical extinction simulations were carried out using the OPPDIF application in CHEMKIN-PRO [41]. The solver uses an arc length continuation method to generate an S-CURV [42] . A detailed chemical kinetic model for n- and iso-butane by Healy et al. [43-45] was used for simulation. Although not all shown here, two other models (i.e., Aramco Mech. 1.3 [46] and 2.0 [47] were tested). The ozone chemistry subset developed by Ombrello et al. [48] with an update from [28, 49] was incorporated into the above models for simulation. The adaptive gradient and curvature limits were set at 0.05 and 0.1, respectively. All simulation results were tested for grid-independence.

2-1 The mass spectrometer

Figure 2a shows a schematic diagram of the mass spectrometer. It comprises of a sampling system, an ion source, a mass analyser and a detector all maintained under high vacuum condition between 10^{-5} and 10^{-8} torr [50]. A modified Hiden HPR-60 MBMS connected to a

Kore time-of-flight (TOF) mass spectrometer (200 *m/z* range) was used to measure species profiles as a function of distance from the fuel nozzle. A 200 mm long quartz sampling probe with an orifice diameter of 0.1 mm was used to collect the sample between the two nozzles. The sampling system of the MBMS consists of three stages held at different pressure. The skimmer cones for the first and second stages are made up of nickel with 0.3mm and 2mm orifice respectively and an external angle of 34 degrees. The first stage is held at a pressure near 10^{-3} Torr by a turbo-molecular pump (Edwards iXR2206, 2200 l/s), while the pressure in the second and third stage is kept near 10^{-7}-10^{-8} and 10^{-8} Torr, respectively, using a turbo-molecular pump (Edwards nEXT240DX) with a pumping speed of 240 l/s in both pumps [51, 52]. Ionization of the sample is achieved using the method of electron impact (EI) which consists of a beam of electrons hitting the gaseous sample and removing an electron from the molecule [53]. The source for this type of ionization is a heated filament which emits electrons, and after that, they are accelerated towards an anode to impact the sample. The charged particles are accelerated by means of an electric field with an energy E=qV (q: charge of the particle, V: applied voltage).

The time of flight mass analyser works by measuring the time taken for the ions to fly through a field free region of known length. Thus, the ions could be distinguished by their mass over a charge (m/z) ratio [50]. The time-of-flight, showed in Fig. 2b, is a tube with a length of 1 m within which the ions will be firstly accelerated by a defined voltage, then they will travel through a field free region; after this, each ion will be slowed down inside a reflectron, made by several rings of increasing potential and send back to the detector, situated on the same side of the ion source. The detector is a secondary electron multiplier (SEM) which considers the electrons emitted after the impact of ions against its surface. The ionization energy is 20eV and the mass resolution is 3500 m/Δm. The output consists of a spectrum *m/z* vs. *Intensity*.

3. Results and Discussion

Self-sustained cool diffusion flames were established for the tested fuels. Figure 3a shows a direct photography of a cool diffusion flame using a digital camera, Nikon D750. The flame was established at 5.02wt% ozone in the oxidizer stream and strain rate of 51 s^{-1}. To further distinguish the cool flame from a hot flame, Fig. 3b shows a picture of a hot flame initiated from the pre-existing cool diffusion flame using an external ignition source. The hot flame is characterized by a bright yellow radiation of soot particles from the flame. Initiation of cool

flames of both fuels was attempted in the absence of ozone; however, as anticipated by Reuter et al. [28], no cool flame could be observed experimentally without the addition of ozone for these fuels.

3-1 Initiation and extinction limits of n-butane and iso-butane

The initiation limits of cool flames were experimentally determined at various strain rates. Tests were carried out to investigate the influence of changing strain rate on the minimum fuel mole fraction required for cool flame initiation. The tests were performed while the temperature of the fuel stream was maintained at 570K (±5K). Figure 4 shows the initiation boundaries of n-butane and iso-butane cool flames. Two borders are visible from the graph; an unstable cool flame and a cool flame, which becomes stable with increasing fuel mole fraction. Typically, an unstable flame is weak and hardly remains sustained for more than 3 seconds. The graph shows that cool flame initiation is favored at low to moderate strain rates. Lower fuel mole fraction is required to initiate the flame at lower strain rates. This is in agreement with previous cool flame studies in counterflow diffusion systems by Won et al. [25], Deng et al. [15] and Reuter et al. [28]. The thickness of the mixing layer and flow residence time decrease as strain rate increases, and this decreases radical diffusion and reacting time scales. Thus, higher fuel mole fraction is required to initiate the cool flame. Also, it is evident from Fig. 4 that n-butane is more reactive than iso-butane at low temperature, which is attributed to the differences in their molecular structure.

Cool diffusion flame initiation was found to be sensitive to the temperature at the outlet of the fuel duct. For this reason, we measured the mole fraction required to establish a cool flame for n-butane at different fuel outlet temperatures. Figure 5 shows that the mole fraction of fuel needed to establish a stable cool diffusion flame decreases with an increase in fuel stream temperature, which can be attributed to increasing cool flame chemical reaction rates with increasing temperature.

3-2 Extinction limits of n-butane and iso-butane cool diffusion flames

The extinction limits of butane cool diffusion flames (represented by fuel extinction mole fraction) were measured as a function of strain rate at a constant temperature and various ozone concentrations. Cool flames were extinguished by decreasing fuel mole fraction after a fully developed flame was established. To extinguish a flame at a particular strain rate and separation

distance, the fuel mole fraction is gradually decreased alongside increasing the nitrogen mole fraction. Therefore, the total mass flow rate will change which will require a change in velocity to maintain a balanced momentum. The fuel mole fraction at extinction was recorded at various strain rates. Figure 6 shows the extinction limits of n-butane and iso-butane cool flames. The result shows that at low strain rates, less fuel is required to sustain the cool diffusion flames; however, at higher strain rates, higher fuel mole fraction was required for the flame to be sustained. This is because the flame is highly stretched at high strain rates due to the high-velocity gradient. Highly strained flame caused most of the generated radicals to escape from the reaction zone, which requires that fuel mole fraction be increased to sustain the flame. Iso-butane showed a lower extinction limit than n-butane, which again is associated to the influence of molecular structure on the low-temperature reactivity of the tested fuels.

3-3 Numerical Results and discussion

As mentioned above, numerical simulations were performed using CHEMKIN-PRO. Although not all shown here, three chemical kinetic models were initially tested to see their capability in predicting the extinction limits of n-butane; Healy et al. [43], Aramco Mech. v1.3 [46] and Aramco Mech. v2.0 [47]. However, the later model was not giving a converging solution and Healy et al. model compared with the experimental data better than Aramco Mech. v1.3 (Fig. S1, supplementary material). Therefore, Healy et al. model was used for subsequent simulations and kinetic analysis. Two ozone sub-models were initially tested; Ombrello et al. [48] with updates by [49] and Princeton high-pressure ozone mechanism also used by [26]. Ombrello et al. sub-model was also used for cool diffusion flames simulations by Won et al. [25], Reuter et al. [28] and Masurier et al. [54], and was shown to perform better (Fig. S2, supplementary material); therefore, it was adopted here for simulation.

Figure 7a and Fig. 7b, respectively, show the comparison of the predicted extinction limits for n-butane and iso-butane by the model against the experimental data. The model captured the experimental trend but over-predicted the extinction limits by up to a factor of two for n-butane and factor of three for iso-butane. This is not surprising, as all previous studies of cool flames in diffusion flames showed a similar outcome [25, 28, 29], indicating that the existing chemical kinetic models (the base chemistry or the ozone sub chemistry) cannot accurately describe the cool flame behavior in a diffusive system despite their ability to reproduce many homogeneous

experiments at low temperatures [43]. As pointed out by Reuter et al. [28], the possible reasons for the inability of these models to accurately predict the cool diffusion flame behavior is that the models are usually validated against ignition delay time and speciation data from established 0-D experiments such as ST, RCM, and JSR. Because of the long ignition delay time of fuels (especially butane) at low temperature, there is a high possibility of deviation from adiabatic and/or homogenous conditions, which is an important assumption in modeling these systems. Experiments in jet stirred reactors are carried out at high fuel dilution, which means that heat release and fuel oxidation could be decoupled. Therefore, it is possible that kinetic models derived from JSR, ST, and RCM can reproduce species data from 0-D homogeneous reactors, but unable to predict flame properties such as extinction, autoignition and flame speeds in transport affected environment. The Healy et al. [43] model was developed for C1-C4-based hydrocarbon and oxygenated fuels, but not yet validated for butane isomers in counterflow diffusion flames.

Brute force sensitivity analyses were carried out on both fuels to see which reactions contribute most to the extinction limits of the cool diffusion flames. These analyses were performed by perturbation of the rate constant coefficients at 5.02wt% ozone addition. The result is presented in Fig. 8. Similar to the previous analysis of large hydrocarbons [25], the present sensitivity analysis reveals that cool diffusion flames are largely sensitive to low-temperature reactions and reactions involving ozone. Dominant reactions include the reactions of alkylperoxy ($ROO^{\cdot}$) and hydroperoxyalkyl ($QOOH^{\cdot}$) radicals. Fuel abstraction reactions by OH and O have positive sensitivities on both fuels because they produce alkyl radicals that initiate the low-temperature reactivity. Also, reactions producing ketohydroperoxide; C4H8OOH1-3O2⇔NC4KET13+OH and C4H8OOH-IO2⇔IC4KETII+OH have positive sensitivities as their subsequent decomposition produce most of the low-temperature heat release. Similarly, reactions involving ozone; O3+N2=>O2+O+N2 and O3+O2=>2O2+O both have positive sensitivities as they produce O radicals which initiate the abstraction of fuel. On the other hand, O3+O⇔2O2 show negative sensitivity as it presents a chain termination pathway by consuming an active O radical. The majority of the reactions contributing to the bulk of heat produced are reactions involving ozone and other low temperature chemistry reactions involving the fuel radicals (Fig. S3 & Fig. S4, supplementary material). This also explains the reason why cool diffusion flames of butane

isomers could not be established without ozone addition, as the flame relies on heat release from the reactions of ozone for their stabilization.

It is clear from the above sensitivity analysis that fuel abstraction by OH and O contributes to the reactivity of the models. Motivated by this, the rates of fuel abstraction by O atom were divided by a factor of 3, and the extinction strain rate was simulated at 5.02wt% ozone (Fig. S5, supplementary material). It follows that by decreasing this rate alone, a better comparison with the experimental data could be achieved. Although the above sensitivity analysis showed that low-temperature reactivity is spread over many species, experimental measurement of the rate of ozone decomposition to atomic O and subsequent fuel abstraction by O radicals might improve the ability of this model to predict cool diffusion flame properties.

It is evident from Fig. 6 that n-butane produces stronger cool diffusion flames than iso-butane. Therefore, reaction path flux analysis was carried out to see the reason for the observed trend. Additionally, based on the results of the sensitivity and path flux analysis, mole fraction profiles of some of the important species were compared to understand further why the two isomers have different cool flame extinction limits.

Figures 9a and 9b shows the path flux analyses of n-butane and iso-butane, respectively both at 50% fuel consumption. The analyses show that almost 65% of n-butane fuel undergoes abstraction on the secondary carbon to subsequently produce an alkylperoxy ($ROO^{\cdot}$) radical through the reaction of SC4H9+O2⇔SC4H8O2. Most of these species directly isomerize to produce various hydroperoxyalkyl ($Q^{\cdot}OOH$) radicals. A majority of the remaining 35% of the fuel goes through hydrogen abstraction on the primary carbon to also produce $ROO^{\cdot}$ radicals through the reaction of PC4H9+O2⇔PC4H9O2. Similarly, over 65% of these species directly isomerize to produce various $Q^{\cdot}OOH$ radicals. As could be seen on Fig. 8a, the ultimate fate of most of the hydroperoxyalkyl radicals is to either directly produce formaldehyde (CH_2O), acetaldehydes (CH_3CHO), propionaldehydes (C_2H_5CHO) or to yield OH through reactions involving ketohydroperoxides (KHP).

For iso-butane, ~35% of the fuel undergoes hydrogen abstraction on the tertiary carbon atom to produce alkylperoxy radical. Most of this ($ROO^{\cdot}$) undergoes concerted elimination to yield iso-butene through the reaction of TC4H9O2⇔IC4H8+HO2. According to the analysis on Fig 8b, this reaction has a negative sensitivity, which means it slows the overall reactivity of the fuel.

Although not shown here, iso-butene reacts with atomic oxygen to produce an iso-propyl radical. The reaction is written in the addition direction, which gives beta scission products without forming an intermediate radical [55]. Iso-propyl radical subsequently reacts to give propene through another reaction with negative sensitivity; IC3H7O2⇔C3H6+HO2. Additionally, ~57% of iso-butane fuel is abstracted to produce an iso-butyl radical which subsequently produce an alkylperoxy ($ROO^{\cdot}$) radical through the reaction of IC4H9+O2⇔IC4H9O2. Some of this IC4H9O2 also undergoes concerted elimination to produce iso-butene through the reaction IC4H9O2<=>IC4H8+HO2. This is in contrast with n-butane where most of the alkylperoxy radicals isomerize to $Q^{\cdot}OOH$ radicals. Previous studies [20, 31, 56, 57] have shown that iso-butene and propene lead to dead-end pathways as they produce resonantly stable radical intermediates.

A comparison of the species mole fraction profiles is presented in Fig. 10 for both fuels. Figure 10a shows that n-butane produces higher CH_2O, CH_3CHO, C_2H_5CHO and OH. Previous studies [15, 25, 31, 58] have shown the importance of these radicals to low-temperature heat release. Therefore, it is not surprising that n-butane produces a stronger cool diffusion flame. On the other hand, Fig. 10b shows that iso-butane produces higher mole fractions of the resonantly stable C_3H_5-S, C_3H_5-T, C_3H_6 and HO_2 species. Although not shown here, most the reactions involving these species have negative sensitivity.

The importance of ozone to the initiation of a cool diffusion flame could also be explained by the reaction path flux analysis in Fig. 10. It can be seen that most of the fuel abstraction is by OH radicals and O atoms. Figures 11a and 11b shows that almost all O radicals are directly produced from ozone reactions, while the majority of OH radicals are either produced from reaction directly involving ozone or reactions with O atoms, which are themselves being generated from ozone reactions. These analyses were performed at respective positions of highest mole fractions of O and OH.

4. Structure of n-butane cool diffusion flame

Previous studies by Won et al. [25], Reuter et al. [29] and Deng et al. [15] have used the GC, PLIF, and PMT, respectively, to measure the concentrations as well as the intensities of the species produced from low-temperature cool diffusion flames. In the present study, the structure

of n-butane cool diffusion flame was measured using a time of flight (TOF) mass spectrometer. The sampling was carried out at strain rate 61 s^{-1} and 5.02wt% ozone addition. The intensities of C_4H_{10}, N_2, O_2 and O_3, as well as CH_2O, CH_3CHO, H_2O, and CO_2 are respectively presented on Fig. 12a and Fig. 12b. To compare the species intensities to model prediction, numerical simulations were carried out at conditions identical to the experiment. The predicted mole fractions of these species are presented in Fig. 12c and Fig. 12d.

As indicated by the peak of CH2O profiles, the experimental measurement showed that n-butane cool diffusion flame is located on the oxidizer side, while the model predicted that flame is located near the stagnation plane in the middle of the two outlets. The observed discrepancy could be due to disturbances introduced by the sampling probe or the inability of the kinetic model to accurately predict the flame's location. It is well known that intrusive sampling of flames using a probe causes significant distortions to the flame [59-63]. It can act as a heat sink, and distorts the temperature and species profiles. The surface of the probe may also cause radical recombination, and can result in a significant loss of radicals such as H, O and OH whose lifetime are very short. As recently reviewed by Egolfopoulos et al., [59] the quantitative effect of sampling probe on flow field is not exactly known but according to J. K. Lefkowitz et al. [64] the effect on speciation is approximately equal to the outer diameter of the sampling probe; which is ± 0.8 mm in this case. As a consequence of all these challenges, only species intensities are reported here. Nevertheless, even without the sampling probe, direct visualization of the flame, as well as the study by [25], indicated that cool diffusion flames are located on the oxidizer side of the stagnation plane most likely due to the strong dependence of the flame on heat release from reactions involving ozone. Both the experiment and the model showed that the fuel and oxidizer streams diffuse into each other at the flame location, indicating slow reaction at low temperature. The trends of species profiles on Fig. 12d agree with the experiments except for CO_2. As could be seen from Fig. 12b, the experiments indicated a broader species profiles and a wider reaction zone compared to the model, which is due to slower fuel consumption as shown in Fig. 12a.

To further understand the structure of n-butane cool diffusion flame, the temperature and mole fractions of some important LT species are plotted on Fig. 13. As could be seen, the reaction zone is located close to the stagnation plane; in the middle of the two outlets. The location of the flame is marked by a peak in temperature and CH2O mole fraction. Just before the flame, the

fuel undergoes the low temperature branching pathway where O2QOOH and NC4KET13 are formed and consumed to give the bulk of CH2O. At the flame location, the temperature is slightly higher and QOOH beta scission to form CH2O, OH and C3H6 is favored. As the temperature decreases, i.e., away from the flame, the remaining fuel that diffuses across the stagnation plane reacts again through the LT pathway forming QOOH and O2QOOH, which subsequently react to produce KHP.

5. Conclusion

An experiment was carried out to study the cool diffusion flame behavior of two butane isomers in a counterflow system. Self-sustained cool diffusion flames of both butane isomers through the addition of ozone were affirmed. Ozone-less cool diffusion flames were not observed even at a high fuel mole fraction. The initiation boundaries and extinction limits of cool flames of butane isomers were investigated. First, an unstable cool flame was formed at a lower fuel mole fraction and a stable cool flame was sustained as the fuel mole fraction was increased. Similar to previous cool flame studies of high molecular weight hydrocarbons, the present results showed that establishment and sustenance of cool diffusion flames of butane isomers was favored at low and moderate strain rates with ozone sensitization. Also, the cool flame initiation was found to be sensitive to the temperature of the fuel stream. Results showed that the fuel mole fraction necessary to establish a cool diffusion flame decreases at higher fuel reactant temperatures. Additionally, the results showed that the extinction limits of n-butane cool diffusion flames was higher than n-butane, reflecting the differences in their low temperature reactivities. The effect of an increase in ozone loading on the extinction limit of cool diffusion flames was also tested. Adding more ozone to the oxidizer stream strengthened the cool flame and increased the extinction limits of both fuels.

Numerical simulations were conducted using a detailed model by Healy et al. [43-45], to examine the ability of the model in predicting the cool flame behaviors of butane isomers in the counterflow diffusion flames. Overall, the model captured the trend in the experiments at all strain rates and ozone concentrations, but over-predicted the experiment results by a factor of two and three for n-butane and iso-butane, respectively. Rate constant sensitivity analysis was carried out to see the reactions controlling the cool flame extinction limits of both fuels. It was

observed that the dominant reactions are those involving low-temperature species. Although the sensitivity is spread over many low-temperature reactions, a measurement of the rates of fuel abstraction by oxygen radical might improve the ability of the model in predicting the extinction limits of ozone-assisted cool diffusion flames. The effects of methyl branching on the behavior of n-butane and iso-butane cool diffusion flames were investigated. It has been observed that while the majority of n-butane reacts through the pathways of hydroperoxyalkyl radicals to produce aldehydes, ketohydroperoxide and hydroxyl radicals, iso-butane favors a pathway leading to the formation of iso-butene and propene radicals. Finally, the structure of n-butane cool diffusion flame was examined using a time of flight mass spectrometer. The intensities of formaldehyde, acetaldehyde and other species were measured and compared to model predictions. The model captured the trend in fuel decomposition and species evolution, but could not accurately predict the flame location and the peak values of species.

Acknowledgements

The presented work was supported by Saudi Aramco under the FUELCOM program and by the King Abdullah University of Science and Technology (KAUST) with competitive research funding given to the Clean Combustion Research Center (CCRC). Authors would like to thank Christopher B. Reuter of Mechanical Engineering, Princeton University for his assistance. We appreciate the valuable contributions of Nour Atef and Samah Y. Mohammed of Combustion and Pyrolysis Chemistry Team at KAUST.

References

[1] N. Naser, S.Y. Yang, G. Kalghatgi, S.H. Chung, Relating the octane numbers of fuels to ignition delay times measured in an ignition quality tester (IQT), Fuel 187 (2017) 117-127.
[2] J. Chang, G. Kalghatgi, A. Amer, Y. Viollet, Enabling High Efficiency Direct Injection Engine with Naphtha Fuel through Partially Premixed Charge Compression Ignition Combustion, SAE Technical Paper 2012-01-0677, doi:10.4271/2012-01-0677(2012).
[3] L. Bates, D. Bradley, G. Paczko, N. Peters, Engine hot spots: Modes of auto-ignition and reaction propagation, Combustion and Flame 166 (2016) 80-85.
[4] P. Dai, Z. Chen, S. Chen, Y. Ju, Numerical experiments on reaction front propagation in n-heptane/air mixture with temperature gradient, Proceedings of the Combustion Institute 35 (2015) 3045-3052.
[5] T. Zhang, W. Sun, Y. Ju, Multi-scale modeling of detonation formation with concentration and temperature gradients in n-heptane/air mixtures, Proceedings of the Combustion Institute 36 (2017) 1539-1547.

[6] M.P.B. Musculus, P.C. Miles, L.M. Pickett, Conceptual models for partially premixed low-temperature diesel combustion, Progress in Energy and Combustion Science 39 (2013) 246-283.
[7] V. Sivasankaralingam, V. Raman, M.J.M. Ali, A. Alfazazi, T. Lu, H. Im, S.M. Sarathy, R. Dibble, Experimental and Numerical Investigation of Ethanol/Diethyl Ether Mixtures in a CI Engine, Report No. 0148-7191, SAE Technical Paper, 2016.
[8] P. Dagaut, S.M. Sarathy, M.J. Thomson, A chemical kinetic study of n-butanol oxidation at elevated pressure in a jet stirred reactor, Proceedings of the Combustion Institute 32 (2009) 229-237.
[9] S.M. Burke, W. Metcalfe, O. Herbinet, F. Battin-Leclerc, F.M. Haas, J. Santner, F.L. Dryer, H.J. Curran, An experimental and modeling study of propene oxidation. Part 1: Speciation measurements in jet-stirred and flow reactors, Combustion and Flame 161 (2014) 2765-2784.
[10] S.M. Sarathy, G. Kukkadapu, M. Mehl, T. Javed, A. Ahmed, N. Naser, A. Tekawade, G. Kosiba, M. AlAbbad, E. Singh, S. Park, M.A. Rashidi, S.H. Chung, W.L. Roberts, M.A. Oehlschlaeger, C.-J. Sung, A. Farooq, Compositional effects on the ignition of FACE gasolines, Combustion and Flame 169 (2016) 171-193.
[11] S.M. Sarathy, G. Kukkadapu, M. Mehl, W. Wang, T. Javed, S. Park, M.A. Oehlschlaeger, A. Farooq, W.J. Pitz, C.-J. Sung, Ignition of alkane-rich FACE gasoline fuels and their surrogate mixtures, Proceedings of the Combustion Institute 35 (2015) 249-257.
[12] M.J. Al Rashidi, J.C. Mármol, C. Banyon, M.B. Sajid, M. Mehl, W.J. Pitz, S. Mohamed, A. Alfazazi, T. Lu, H.J. Curran, A. Farooq, S.M. Sarathy, Cyclopentane combustion. Part II. Ignition delay measurements and mechanism validation, Combustion and Flame 183 (2017) 372-385.
[13] A. Alfazazi, M. Sarathy, O.A. Kuti, Modelling Ignition Processes of Palm Oil Biodiesel and Diesel Fuels Using a Two Stage Lagrangian Approach, Report No. 0148-7191, SAE Technical Paper, 2015.
[14] N. Atef, G. Kukkadapu, S.Y. Mohamed, M.A. Rashidi, C. Banyon, M. Mehl, K.A. Heufer, E.F. Nasir, A. Alfazazi, A.K. Das, C.K. Westbrook, W.J. Pitz, T. Lu, A. Farooq, C.-J. Sung, H.J. Curran, S.M. Sarathy, A comprehensive iso-octane combustion model with improved thermochemistry and chemical kinetics, Combustion and Flame 178 (2017) 111-134.
[15] S. Deng, P. Zhao, D. Zhu, C.K. Law, NTC-affected ignition and low-temperature flames in nonpremixed DME/air counterflow, Combustion and Flame 161 (2014) 1993-1997.
[16] F.N. Egolfopoulos, P.E. Dimotakis, Non-premixed hydrocarbon ignition at high strain rates, Symposium (International) on Combustion 27 (1998) 641-648.
[17] a.T. Holley, Y. Dong, M.G. Andac, F.N. Egolfopoulos, T. Edwards, Ignition and extinction of non-premixed flames of single-component liquid hydrocarbons, jet fuels, and their surrogates, Proceedings of the Combustion Institute 31 I (2007) 1205-1213.
[18] C.G. Fotache, H. Wang, C.K. Law, Ignition of ethane, propane, and butane in counterflow jets of cold fuel versus hot air under variable pressures, Combustion and Flame 117 (1999) 777-794.
[19] S.H. Won, S. Dooley, F.L. Dryer, Y. Ju, A radical index for the determination of the chemical kinetic contribution to diffusion flame extinction of large hydrocarbon fuels, Combustion and Flame 159 (2012) 541-551.
[20] S. Mani Sarathy, U. Niemann, C. Yeung, R. Gehmlich, C.K. Westbrook, M. Plomer, Z. Luo, M. Mehl, W.J. Pitz, K. Seshadri, M.J. Thomson, T. Lu, A counterflow diffusion flame study of branched octane isomers, Proceedings of the Combustion Institute 34 (2013) 1015-1023.

[21] X.L. Zheng, T.F. Lu, C.K. Law, C.K. Westbrook, H.J. Curran, Experimental and computational study of nonpremixed ignition of dimethyl ether in counterflow, Proceedings of the Combustion Institute 30 (2005) 1101-1109.
[22] R. Grana, K. Seshadri, A. Cuoci, U. Niemann, T. Faravelli, E. Ranzi, Kinetic modelling of extinction and autoignition of condensed hydrocarbon fuels in non-premixed flows with comparison to experiment, Combustion and Flame 159 (2012) 130-141.
[23] C.K. Law, P. Zhao, NTC-affected ignition in nonpremixed counterflow, Combustion and Flame 159 (2012) 1044-1054.
[24] W. Sun, S.H. Won, Y. Ju, In situ plasma activated low temperature chemistry and the S-curve transition in DME/oxygen/helium mixture, Combustion and Flame 161 (2014) 2054-2063.
[25] S.H. Won, B. Jiang, P. Diévart, C.H. Sohn, Y. Ju, Self-sustaining n-heptane cool diffusion flames activated by ozone, Proceedings of the Combustion Institute 35 (2015) 881-888.
[26] H. Zhao, X. Yang, Y. Ju, Kinetic studies of ozone assisted low temperature oxidation of dimethyl ether in a flow reactor using molecular-beam mass spectrometry, Combustion and Flame 173 (2016) 187-194.
[27] S. Deng, D. Han, C.K. Law, Ignition and extinction of strained nonpremixed cool flames at elevated pressures, Combustion and Flame 176 (2017) 143-150.
[28] C.B. Reuter, M. Lee, S.H. Won, Y. Ju, Study of the low-temperature reactivity of large n-alkanes through cool diffusion flame extinction, Combustion and Flame 179 (2017) 23-32.
[29] C.B. Reuter, S.H. Won, Y. Ju, Experimental study of the dynamics and structure of self-sustaining premixed cool flames using a counterflow burner, Combustion and Flame 166 (2016) 125-132.
[30] C.B. Reuter, S.H. Won, Y. Ju, Flame structure and ignition limit of partially premixed cool flames in a counterflow burner, Proceedings of the Combustion Institute 36 (2016) 1513–1522.
[31] A. Alfazazi, U. Niemann, H.M. Selim, R.J. Cattolica, S.M. Sarathy, Effects of substitution on counterflow ignition and extinction of C3 and C4 alcohols, Energy & Fuels 30 (2016) 6091–6097.
[32] N. Liu, S. Mani Sarathy, C.K. Westbrook, F.N. Egolfopoulos, Ignition of non-premixed counterflow flames of octane and decane isomers, Proceedings of the Combustion Institute 34 (2013) 903-910.
[33] N. Donohoe, A. Heufer, W.K. Metcalfe, H.J. Curran, M.L. Davis, O. Mathieu, D. Plichta, A. Morones, E.L. Petersen, F. Güthe, Ignition delay times, laminar flame speeds, and mechanism validation for natural gas/hydrogen blends at elevated pressures, Combustion and Flame 161 (2014) 1432-1443.
[34] E. Ranzi, T. Faravelli, P. Gaffuri, G.C. Pennatti, A. Sogaro, A Wide Range Modeling Study of Propane and n-Butane Oxidation, Combustion Science and Technology 100 (1994) 299-330.
[35] N.M. Marinov, W.J. Pitz, C.K. Westbrook, M.J. Castaldi, S.M. Senkan, C.F. Melius, Aromatic and Polycyclic Aromatic Hydrocarbon Formation in a Laminar Premixed n-Butane Flame, Combustion and Flame 114 (1998) 192-213.
[36] S. Kojima, Detailed modeling of n-butane autoignition chemistry, Combustion and Flame 99 (1994) 87-136.
[37] T. Ogura, Y. Nagumo, A. Miyoshi, M. Koshi, Chemical Kinetic Mechanism for High Temperature Oxidation of Butane Isomers, Energy & Fuels 21 (2007) 130-135.
[38] V. Warth, N. Stef, P.A. Glaude, F. Battin-Leclerc, G. Scacchi, G.M. Côme, Computer-Aided Derivation of Gas-Phase Oxidation Mechanisms: Application to the Modeling of the Oxidation of n-Butane, Combustion and Flame 114 (1998) 81-102.

[39] A. Chakir, M. Cathonnet, J. Boettner, F. Gaillard, Kinetic study of n-butane oxidation, Combustion science and technology 65 (1989) 207-230.
[40] K. Seshadri, F.A. Williams, Laminar flow between parallel plates with injection of a reactant at high reynolds number, International Journal of Heat and Mass Transfer 21 (1978) 251-253.
[41] Reaction-Design, ANSYS CHEMKIN-PRO, 17.2; Reaction Design: San Diego, CA, 2016, San Diego.
[42] Y. Ju, H. Guo, K. Maruta, F. Liu, On the extinction limit and flammability limit of non-adiabatic stretched methane–air premixed flames, Journal of Fluid Mechanics 342 (1997) 315-334.
[43] D. Healy, D.M. Kalitan, C.J. Aul, E.L. Petersen, G. Bourque, H.J. Curran, Oxidation of C1 - C5 Alkane Quinternary Natural Gas Mixtures at High Pressures, Energy Fuels 24 (2010) 1521-1528.
[44] D. Healy, N.S. Donato, C.J. Aul, E.L. Petersen, C.M. Zinner, G. Bourque, H.J. Curran, Isobutane ignition delay time measurements at high pressure and detailed chemical kinetic simulations, Combustion and Flame 157 (2010) 1540-1551.
[45] D. Healy, N.S. Donato, C.J. Aul, E.L. Petersen, C.M. Zinner, G. Bourque, H.J. Curran, n-Butane: Ignition delay measurements at high pressure and detailed chemical kinetic simulations, Combustion and Flame 157 (2010) 1526-1539.
[46] W.K. Metcalfe, S.M. Burke, S.S. Ahmed, H.J. Curran, A Hierarchical and Comparative Kinetic Modeling Study of C1 − C2 Hydrocarbon and Oxygenated Fuels, International Journal of Chemical Kinetics 45 (2013) 638-675.
[47] Y. Li, C.-W. Zhou, K.P. Somers, K. Zhang, H.J. Curran, The oxidation of 2-butene: A high pressure ignition delay, kinetic modeling study and reactivity comparison with isobutene and 1-butene, Proceedings of the Combustion Institute 36 (2017) 403-411.
[48] T. Ombrello, S.H. Won, Y. Ju, S. Williams, Flame propagation enhancement by plasma excitation of oxygen. Part I: Effects of O3, Combustion and Flame 157 (2010) 1906-1915.
[49] Y. Ju, W. Sun, Plasma assisted combustion: Dynamics and chemistry, Progress in Energy and Combustion Science 48 (2015) 21-83.
[50] J.H. Gross, Mass spectrometry: a textbook, Springer Science & Business Media2006.
[51] A.B.S. Alquaity, J. Han, M. Chahine, H. Selim, M. Belhi, S.M. Sarathy, F. Bisetti, A. Farooq, Measurements of Positively Charged Ions in Premixed Methane-Oxygen Atmospheric Flames, Combustion Science and Technology 189 (2017) 575-594.
[52] A.B.S. Alquaity, B. Chen, J. Han, H. Selim, M. Belhi, Y. Karakaya, T. Kasper, S.M. Sarathy, F. Bisetti, A. Farooq, New insights into methane-oxygen ion chemistry, Proceedings of the Combustion Institute 36 (2017) 1213-1221.
[53] J.C. Lindon, G.E. Tranter, D. Koppenaal, Encyclopedia of spectroscopy and spectrometry, Academic Press2016.
[54] J.-B. Masurier, F. Foucher, G. Dayma, P. Dagaut, Investigation of iso-octane combustion in a homogeneous charge compression ignition engine seeded by ozone, nitric oxide and nitrogen dioxide, Proceedings of the Combustion Institute 35 (2015) 3125-3132.
[55] S.M. Sarathy, C.K. Westbrook, M. Mehl, W.J. Pitz, C. Togbe, P. Dagaut, H. Wang, M.a. Oehlschlaeger, U. Niemann, K. Seshadri, P.S. Veloo, C. Ji, F.N. Egolfopoulos, T. Lu, Comprehensive chemical kinetic modeling of the oxidation of 2-methylalkanes from C7 to C20, Combustion and Flame 158 (2011) 2338-2357.

[56] P.S. Veloo, F.N. Egolfopoulos, Flame propagation of butanol isomers/air mixtures, Proceedings of the Combustion Institute 33 (2011) 987-993.
[57] P.S. Veloo, F.N. Egolfopoulos, Studies of n-propanol, iso-propanol, and propane flames, Combustion and Flame 158 (2011) 501-510.
[58] A. Alfazazi, O.A. Kuti, N. Naser, S.H. Chung, S.M. Sarathy, Two-stage Lagrangian modeling of ignition processes in ignition quality tester and constant volume combustion chambers, Fuel 185 (2016) 589-598.
[59] F.N. Egolfopoulos, N. Hansen, Y. Ju, K. Kohse-Höinghaus, C.K. Law, F. Qi, Advances and challenges in laminar flame experiments and implications for combustion chemistry, Progress in Energy and Combustion Science 43 (2014) 36-67.
[60] J.C. Biordi, Molecular beam mass spectrometry for studying the fundamental chemistry of flames, Progress in Energy and Combustion Science 3 (1977) 151-173.
[61] U. Struckmeier, P. Oßwald, T. Kasper, L. Böhling, M. Heusing, M. Köhler, A. Brockhinke, K. Kohse-Höinghaus, Sampling probe influences on temperature and species concentrations in molecular beam mass spectroscopic investigations of flat premixed low-pressure flames, Zeitschrift für Physikalische Chemie 223 (2009) 503-537.
[62] A.T. Hartlieb, B. Atakan, K. Kohse-Höinghaus, Effects of a sampling quartz nozzle on the flame structure of a fuel-rich low-pressure propene flame, Combustion and flame 121 (2000) 610-624.
[63] N. Hansen, T.A. Cool, P.R. Westmoreland, K. Kohse-Höinghaus, Recent contributions of flame-sampling molecular-beam mass spectrometry to a fundamental understanding of combustion chemistry, Progress in Energy and Combustion Science 35 (2009) 168-191.
[64] J.K. Lefkowitz, S.H. Won, Y. Fenard, Y. Ju, Uncertainty assessment of species measurements in acetone counterflow diffusion flames, Proceedings of the Combustion Institute 34 (2013) 813-820.
[65] K.G. Standing, E. Warner, Time of Flight Mass Spectrometers, Encyclopedia of Spectroscopy and Spectrometry, 1999.

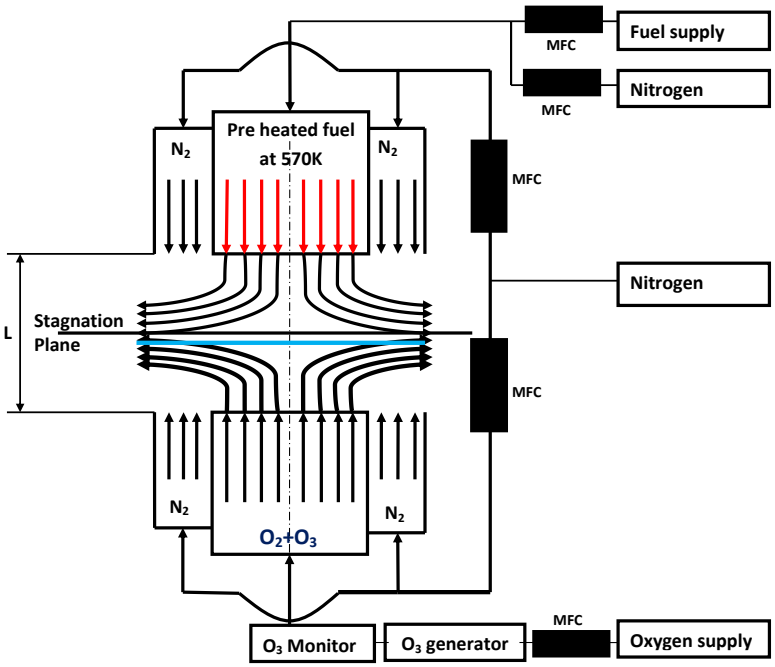

Figure 1. An illustration of the counterflow facility

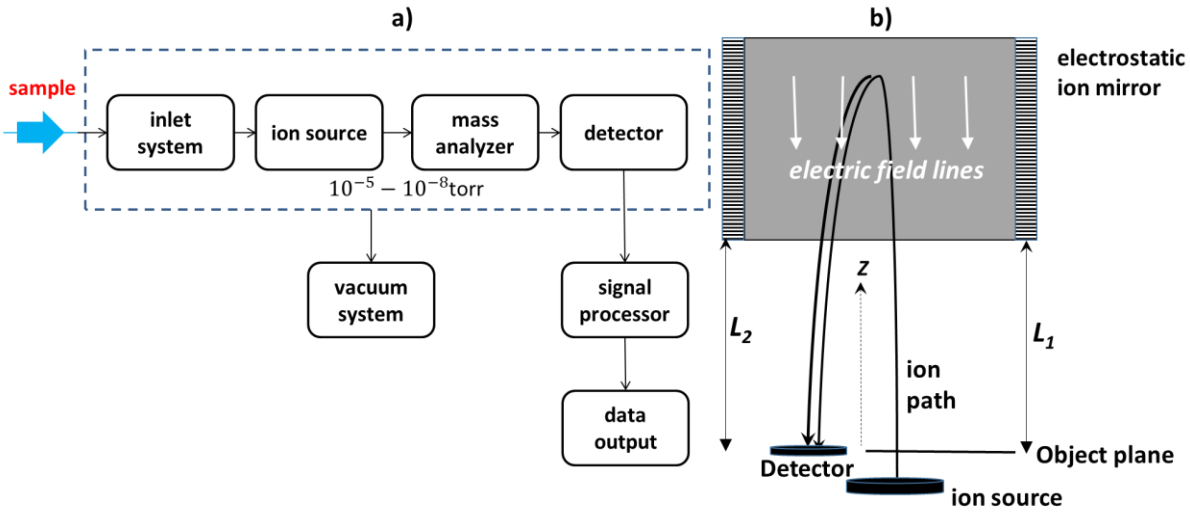

Figure 2. a) Block scheme of a mass spectrometer b) Illustration of an electrostatic ion mirror or reflectron [65]

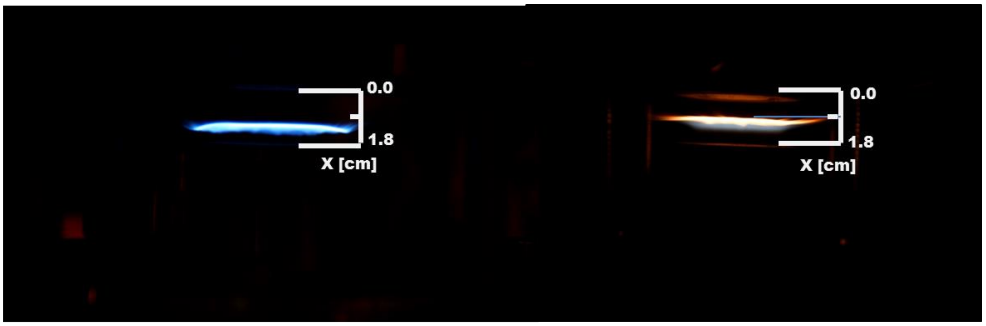

Figure 3. Direct photography of n-butane a) cool flame initiated by ozone addition b) hot diffusion flame from the pre-existing cool diffusion flame at 5.02wt% ozone. Strain rate 51 s^{-1}.

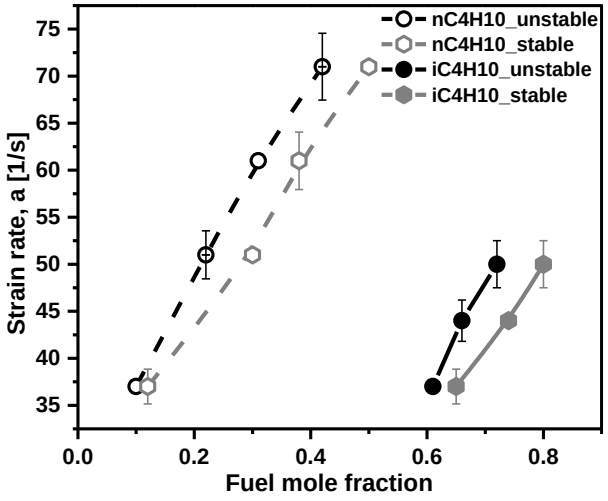

Figure 4. Initiation limits of cool diffusion flame. Fuel mole fractions required for establishment of cool diffusion flames at various strain rates and 5.02wt % ozone on the oxidizer stream. Fuel side temperature T_F=570K. Opened and closed symbols represent n-butane (nC4H10) and iso-butane (iC4H10) initiation limits, respectively.

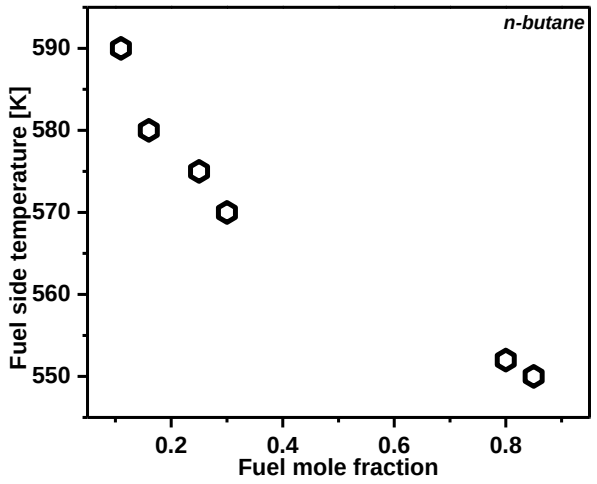

Figure 5. Mole fraction of fuel required to initiate a stable cool diffusion flame at various fuel side outlet temperatures and 5.02wt% ozone. Strain rate = 51 s^{-1}.

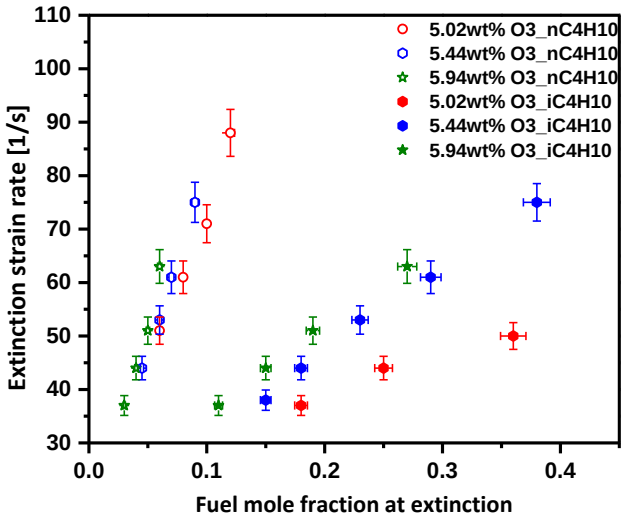

Figure 6. Cool diffusion flame extinction limits at various strain rates and ozone concentrations. Fuel side temperature, T_F= 570K.

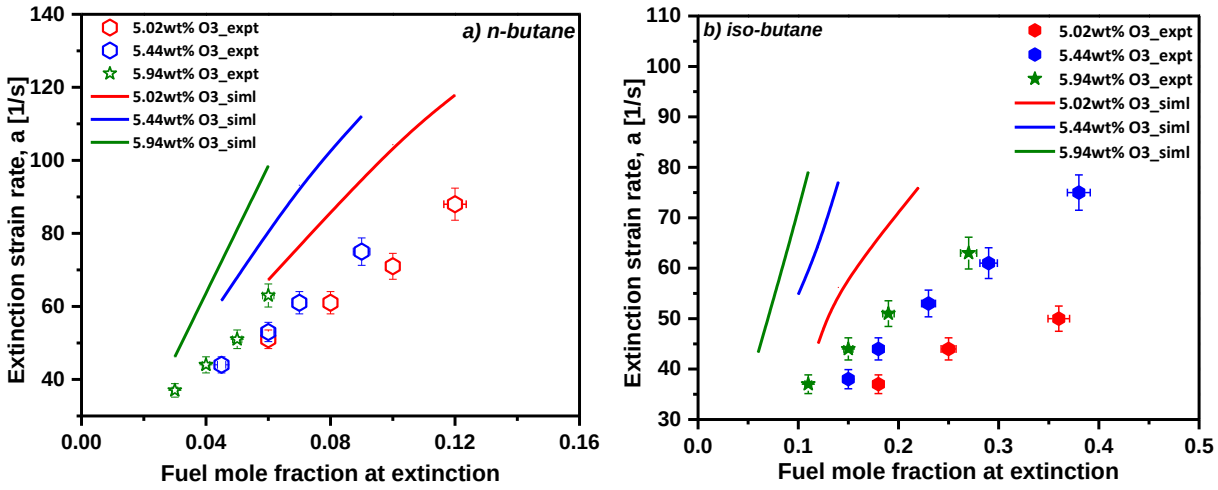

Figure 7. Comparison of measured and computed extinction limits of a) n-butane b) iso-butane cool flames as a function of strain rates with three different levels of ozone addition. Fuel side temperature T_F=570K.

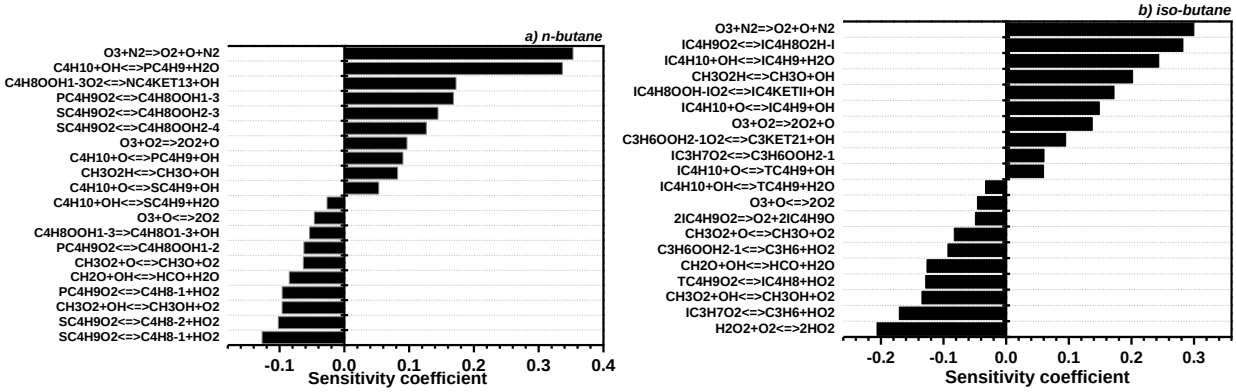

Figure 8. Rate constant sensitivity analyses for extinction strain rate of a) n-butane b) iso-butane cool diffusion flame at 5.68wt% ozone. T_F = 570K.

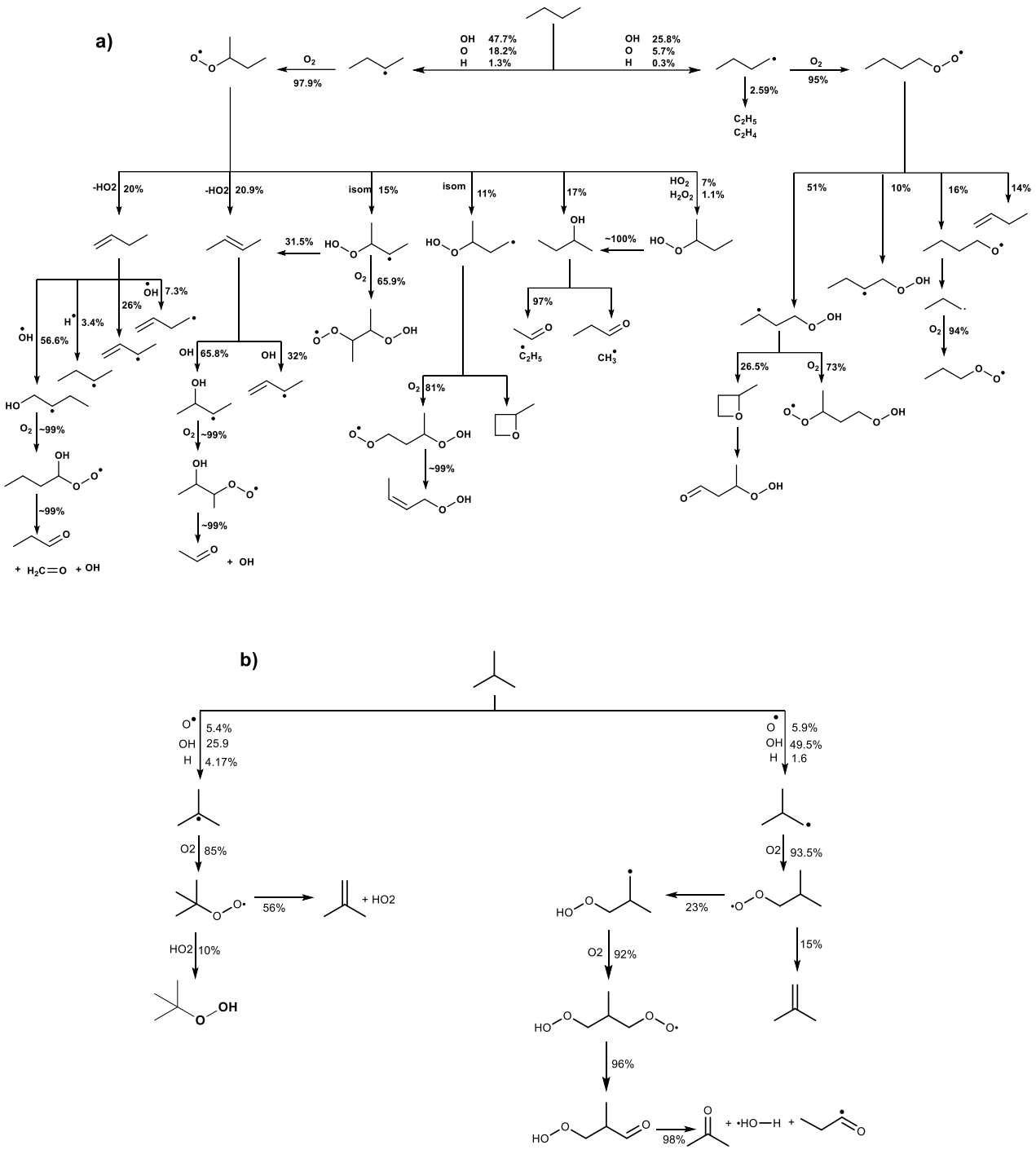

Figure 9. Reaction path flux analysis at 50% fuel consumption showing the major pathways for decomposition of a) n-butane b) iso-butane fuels at 5.02wt% ozone addition and 51 s^{-1}. Numbers indicate consumption percentage

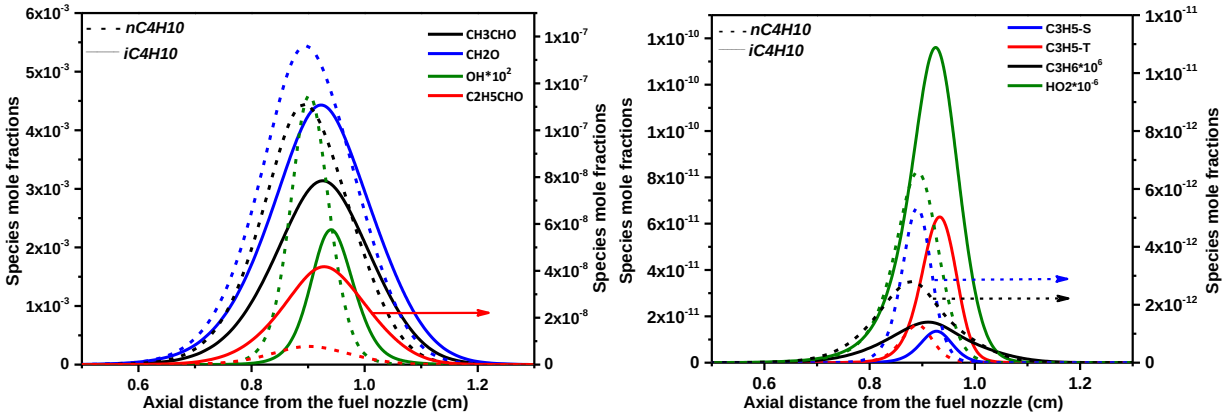

Figure 10. Comparison of the species profiles from the oxidation of n-butane (dash lines) and iso-butane (solid lines) fuels at 5.02wt% ozone addition and 51 s^{-1}. Arrows on profiles indicates corresponding right axis readings

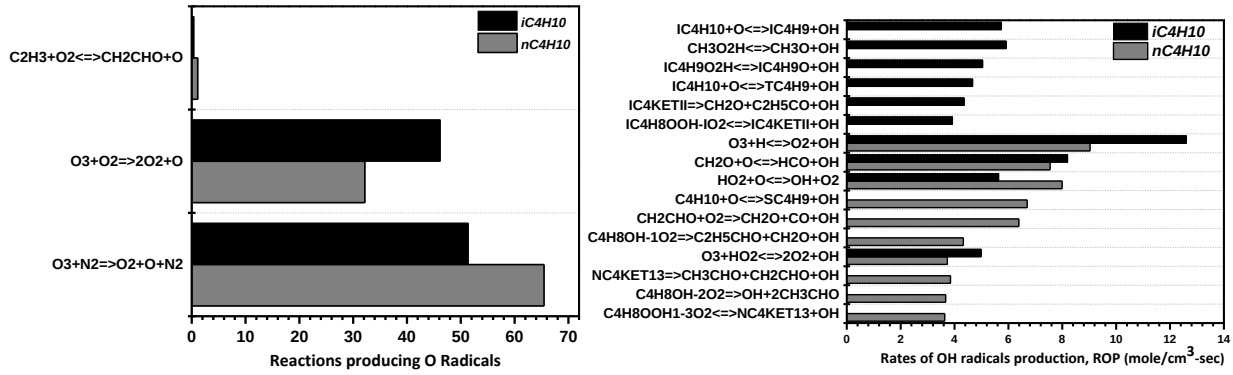

Figure 11. Reaction path flux analysis showing the main reaction pathways for the production of O and OH radicals at 5.02wt% ozone addition and 51 s^{-1}. Analyses were carried out at locations of maximum O and OH mole fractions.

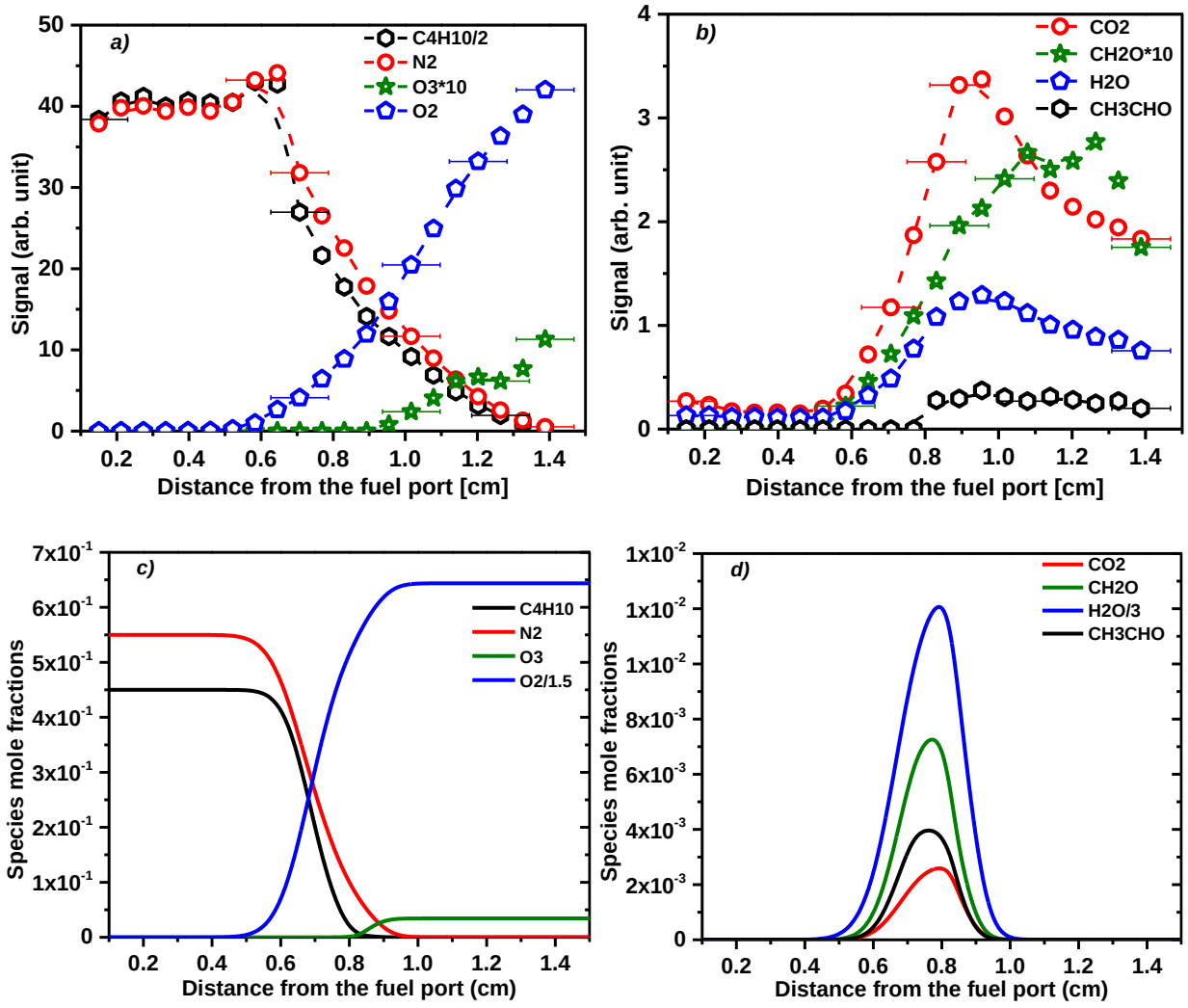

Figure 12. Structure of n-butane cool diffusion flame at strain rate 61 s^{-1} and 5.02wt% ozone addition. Symbols in (a) and (b) represent experimental measurements and lines in (c) and (d) are model predictions

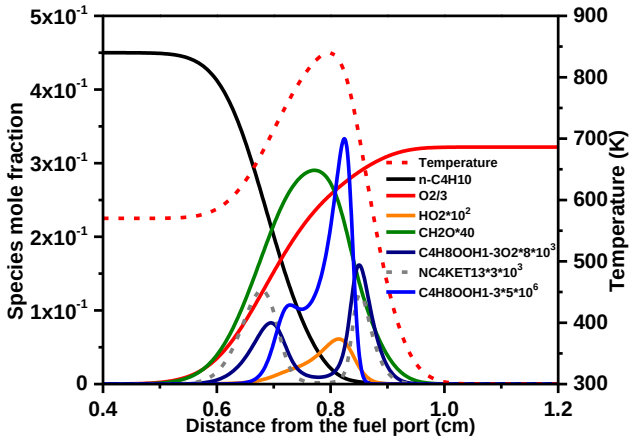

Figure 13. Simulated structure of n-butane cool diffusion flame at conditions identical to Fig. 13